THE FASEB JOURNAL • RESEARCH • www.fasebj.org

Calorie restriction prevents diet-induced insulin resistance independently of PGC-1-driven mitochondrial biogenesis in white adipose tissue

Rosario Pardo,[*,1] Maria Vilà,[*,1] Luis Cervela,[*] Marina de Marco,[*] Pau Gama-Pérez,[†] Alba González-Franquesa,[†,2] Lucia Statuto,[*] Ramon Vilallonga,[*,‡] Rafael Simó,[§,¶] Pablo M. Garcia-Roves,[†] and Josep A. Villena[*,¶,3]

[*]Laboratory of Metabolism and Obesity and [§]Unit of Diabetes and Metabolism, Vall d'Hebron-Institut de Recerca, Universitat Autònoma de Barcelona, Barcelona, Spain; [†]Department of Physiological Sciences, Institut d'Investigació Biomèdica de Bellvitge, Universitat de Barcelona, L'Hospitalet de Llobregat, Barcelona, Spain; [‡]Metabolic and Bariatric Surgery Unit, European Accreditation Council for Bariatric Surgery Center of Excellence, Vall d'Hebron University Hospital, Barcelona, Spain; and [¶]Centro de Investigación Biomédica en Red de Diabetes y Enfermedades Metabólicas Asociadas, Instituto de Salud Carlos III, Barcelona, Spain

ABSTRACT: Calorie restriction (CR) exerts remarkable, beneficial effects on glucose homeostasis by mechanisms that are not fully understood. Given the relevance of white adipose tissue (WAT) in glucose homeostasis, we aimed at identifying the main cellular processes regulated in WAT in response to CR in a pathologic context of obesity. For this, a gene-expression profiling study was first conducted in mice fed *ad libitum* or subjected to 40% CR. We found that the gene network related to mitochondria was the most highly upregulated in WAT by CR. To study the role that increased mitochondrial biogenesis plays on glucose homeostasis following CR, we generated a mouse model devoid of the coactivators peroxisome proliferator-activated receptor γ coactivator 1 (PGC-1)α and PGC-1β specifically in adipocytes. Our results show that mice lacking PGC-1s in adipocytes are unable to increase mitochondrial biogenesis in WAT upon CR. Despite a blunted induction of mitochondrial biogenesis in response to calorie deprivation, mice lacking adipose PGC-1s still respond to CR by improving their glucose homeostasis. Our study demonstrates that PGC-1 coactivators are major regulators of CR-induced mitochondrial biogenesis in WAT and that increased mitochondrial biogenesis and oxidative function in adipose tissue are not required for the improvement of glucose homeostasis mediated by CR.—Pardo, R., Vilà, M., Cervela, L., de Marco, M., Gama-Pérez, P., González-Franquesa, A., Statuto, L., Vilallonga, R., Simó, R., Garcia-Roves, P. M., Villena, J. A. Calorie restriction prevents diet-induced insulin resistance independently of PGC-1-driven mitochondrial biogenesis in white adipose tissue. FASEB J. 33, 2343–2358 (2019). www.fasebj.org

KEY WORDS: oxidative metabolism · adipocytes · glucose homeostasis · mitochondria

Dysregulation of white adipose tissue (WAT) function, as it occurs in obesity, is associated with a variety of metabolic derangements, including insulin resistance, glucose intolerance, hyperlipidemia, and hepatic steatosis (1). These metabolic alterations lie beneath the development of severe obesity-associated comorbidities, such as cardiovascular disease, certain types of cancer, and type 2 diabetes (T2D), which result in increased morbidity and

ABBREVIATIONS: ACO2, aconitase 2; AKT, protein kinase B; AL, *ad libitum*; Arg1, arginase 1; ATP5b, mitochondrial ATP synthetase β subunit; BAT, brown adipose tissue; CIDEA, cell death-inducing DNA fragmentation factor α-like effector A; COL, collagen; COXII, cytochrome C oxidase subunit II; COXIV, cytochrome C oxidase subunit IV; CR, calorie restriction; CYPA, cyclophilin A; ECM, extracellular matrix; ETS, electron-transfer system; FCCP, carbonylcyanide-4-(trifluoromethoxy)-phenyl-hydrazone; GO, gene ontology; GTT, glucose tolerance test; HF, high fat; ITT, insulin tolerance test; M1, classically activated macrophages; M2, alternatively activated macrophages; mtDNA, mitochondrial DNA; NDUFB9, NADH:ubiquinone oxidoreductase subunit B9; oxphos, oxidative phosphorylation; PGC-1, peroxisome proliferator-activated receptor γ coactivator 1; PGC-1α/β-FAT-DKO, peroxisome proliferator-activated receptor γ coactivator 1α/β double-knockout mice; *Ppargc*, peroxisome proliferator-activated receptor γ coactivator; qRT-PCR, quantitative RT-PCR; SDHB, succinate dehydrogenase complex subunit B; Sirt1, Sirtuin 1; T2D, type 2 diabetes; TZD, thiazolidinedione; UCP1, uncoupling protein 1; WAT, white adipose tissue; WT, wild type

[1] These authors contributed equally to this work.

[2] Current affiliation: The Novo Nordisk Center for Basic Metabolic Research, Københavns Universitet, Copenhagen, Denmark.

[3] Correspondence: Laboratory of Metabolism and Obesity, Unit of Diabetes and Metabolism, Vall d'Hebron-Institut de Recerca, Passeig Vall d'Hebron, 119-129, Barcelona 08035, Spain. E-mail: josep.villena@vhir.org

doi: 10.1096/fj.201800310R

This article includes supplemental data. Please visit *http://www.fasebj.org* to obtain this information.

mortality among obese individuals. In this regard, the prevalence of T2D has grown steadily in close association with the rise of obesity, and currently, T2D has become a major health problem of epidemic proportions (2).

As a key endocrine and lipid storage organ, WAT plays a central role in the control of glucose homeostasis. In an obesogenic environment, reduced energy expenditure and excessive calorie intake favor the accumulation of triglycerides in WAT, ultimately leading to hypertrophic and dysfunctional adipocytes. Several cellular processes in WAT contribute to adipocyte-specific and whole-body insulin resistance. For example, sustained nutrient overload of adipocytes in obese subjects results in an altered endocrine function and the inability of fat cells to store lipids further in an efficient manner, leading to ectopic lipid deposition and impaired insulin signaling (3). Interestingly, mitochondrial dysfunction has also been suggested to contribute to insulin resistance by favoring the accumulation of lipid intermediates that disrupt proper insulin signaling (4). In addition, activation in hypertrophic adipocytes of stress signaling pathways, such as endoplasmic reticulum stress, enhanced reactive oxygen species production, or hypoxic responses, results in increased cell death and triggers a chronic low-degree inflammatory response in WAT characterized by increased recruitment of immune cells, enhanced macrophage polarization toward the classically activated macrophages (M1) proinflammatory type, and augmented secretion of proinflammatory cytokines (5). The secretion of inflammatory cytokines (*e.g.*, TNF-α, IL-1β, IL-6) by both adipocytes and infiltrated macrophages leads to the activation of the JNK and IKK-NF-κB pathways that directly impair insulin signal transduction and cause insulin resistance (6). Although numerous studies have provided compelling evidence that supports a role of adipose lipotoxicity and inflammation in the pathogenesis of insulin resistance, the contribution of other processes, such as impaired mitochondrial function, remains to be elucidated.

Nutritional interventions have proven very efficient in reducing excessive fat accumulation and reverting obesity-associated diseases, including insulin resistance. Calorie restriction (CR), defined as a 20–50% reduction in calorie intake, is the only lifestyle intervention known to extend lifespan in a wide variety of species, from yeast to primates (7). The mechanisms by which CR delays aging are not fully understood, but the remarkable effects that CR has on health—delaying the onset and progression of numerous pathologies, including insulin resistance and T2D—may contribute to extend a lifespan. In this regard, given the difficulty of patients to adhere to a long-term CR regime, the identification of the mechanisms and processes that mediate the beneficial effects of CR is crucial for the identification of new target molecules and the development of new therapies based on drugs that mimic CR. However, the key processes modulated by CR in WAT have not been fully characterized, and their relevance with regard to the control of glucose homeostasis remains to be defined.

In this study, we have performed a gene-expression profiling analysis in WAT of mice subjected to CR and identified mitochondrial biogenesis as the most upregulated process in response to CR. With the consideration of the tight correlation between mitochondrial mass and insulin sensitivity reported in humans and animal models [reviewed in Zamora and Villena (8)], we aimed at investigating first, the mechanisms that regulate mitochondrial biogenesis in response to CR and second, whether the increase in mitochondrial mass and oxidative function in WAT is necessary for the improvement in glucose homeostasis exerted by CR.

MATERIALS AND METHODS

Animal studies

Adipose-specific peroxisome proliferator-activated receptor γ coactivator 1 (PGC-1)α/PGC-1β double-knockout mice (PGC-1α/β-FAT-DKO) were obtained by crossing double-homozygous peroxisome proliferator-activated receptor γ coactivator (*Ppargc*)*1a*$^{flox/flox}$, *Ppargc1b*$^{flox/flox}$ mice with transgenic mice expressing Cre recombinase under the control of the adipocyte-specific adiponectin promoter (AdipoQ-Cre) (9). The generation of *Ppargc1a*$^{flox/flox}$ and *Ppargc1b*$^{flox/flox}$ mice has been previously described, and mice had been backcrossed for at least 10 generations with C57BL6/J mice to ensure a homogeneous genetic background (10, 11). Mice were housed in a temperature-controlled environment at 21°C, subjected to a 12/12 h light/dark cycle and fed a standard diet (2018 Tecklad Global 18% Protein Rodent Diet; Harlan Laboratories, Indianapolis, IN, USA), unless otherwise stated. In all experiments, Cre-negative PGC-1α/β-FAT-DKO littermates were used as wild-type (WT) controls. For the gene-expression profiling study, WT C57BL6/J male mice were used.

For the CR experiments, all mice were individually caged and started receiving a high-fat (HF) diet (45% kcal fat, 35% kcal carbohydrates, 20% kcal protein; Research Diets, New Brunswick, NJ, USA) at the age of 7 wk. At the age of 8 wk, mice were randomly assigned to *ad libitum* (AL) or CR groups. During the following week, CR animals received 80% of the food eaten by their AL counterparts. Afterwards, CR mice started receiving 60% of the food eaten by AL animals. Mice were subjected to 40% CR for a period of 12 wk.

All procedures involving animals were conducted according to the European Union Ethical Guidelines and approved by the Animal Experimentation and Ethics Committee of Vall d'Hebron Research Institute (12/11 CEEA).

Microarray analysis

Gene-expression profiling in WAT of AL and CR mice was performed as previously described (12). In brief, total RNA was isolated from inguinal WAT of C57BL6/J WT mice fed AL or subjected to CR (n = 5) with Trizol reagent, further purified using the RNeasy Mini kit (Qiagen, Germantown, MD, USA) and then used to synthesize sense single-stranded DNA with the Ambion WT Expression kit (Thermo Fisher Scientific, Waltham, MA, USA), following the manufacturer's instructions. Labeled single-stranded DNA was hybridized onto Mouse Gene 1.0 ST arrays (Thermo Fisher Scientific). The arrays were scanned, and the resulting images were processed with the Microarray Analysis Suite 5.0 software package (Thermo Fisher Scientific). The data obtained were analyzed by the Unit of Statistics and Bioinformatics from the Vall d'Hebron Research Institute (Barcelona, Spain) using Bioconductor software (*https://www.bioconductor.org/*) to generate a list of genes differentially expressed in WAT of

CR mice. A gene-enrichment analysis was performed using the Database for Annotation, Visualization and Integrated Discovery (DAVID) Bioinformatics Database functional annotation tool (*https://david.ncifcrf.gov/summary.jsp*) (13) and the Gene Set Enrichment Analysis (GSEA) method (*http://software.broadinstitute.org/gsea/index.jsp*) (14) to identify the main biologic processes and gene networks regulated by CR in WAT.

Real-time quantitative RT-PCR

Total RNA was used to synthesize cDNA with SuperScript II RT (Thermo Fisher Scientific) and oligo-dT. Gene expression was determined by real-time quantitative RT-PCR (qRT-PCR) using SYBR green dye and gene-specific primers as described in Pardo *et al.* (11).

Western blot

Protein extracts from inguinal WAT or interscapular brown adipose tissue (BAT) were prepared in homogenization buffer (50 mM Tris-HCl, 150 mM NaCl, 1% Nonidet P-40, 5 mM EGTA, 5 mM EDTA, 1 mM PMSF) containing protease inhibitors. WAT or BAT protein extracts (15–30 μg) were subjected to electrophoresis in a 12% or 15% SDS-PAGE and transferred to a PVDF membrane. Immunodetection was performed with specific antibodies against aconitase 2 (ACO2; ab71440, 1:1000; Abcam, Cambridge, United Kingdom), cytochrome C oxidase subunit IV (COXIV; 4844, 1:1000; Cell Signaling Technology, Danvers, MA, USA), succinate dehydrogenase complex subunit B (SDHB; ab84622, 1:1000; Abcam), NADH:ubiquinone oxidoreductase subunit B9 (NDUFB9; ab106699, 1:1000; Abcam), mitochondrial ATP synthetase β subunit (ATP5b; ab85068, 1:1000; Abcam), α-tubulin (11H10, 1:1000; Cell Signaling Technology), and cyclophilin A (CYPA; BML-SA296, 1:5000; Enzo Life Sciences, Farmingdale, NY, USA). For detection of uncoupling protein 1 (UCP1; ab10983, 1:3000 Abcam), protein extracts (50 μg) from inguinal WAT were used. Horseradish peroxidase-conjugated goat anti-rabbit-purified IgG was used as a secondary antibody (172-1013, 1:10,000; Bio-Rad, Hercules, CA, USA).

Mitochondrial DNA content

Relative quantification of mitochondrial DNA (mtDNA) in WAT was performed by qRT-PCR using 2 ng total DNA as a template and specific primers to amplify cytochrome C oxidase subunit II (COXII; mtDNA) and receptor-interacting protein 140 (nuclear DNA). The detailed procedure has been described in Villena *et al.* (15).

High-resolution respirometry

Mitochondrial respiration was assessed in freshly isolated WAT by high-resolution respirometry in an Oroboros Oxygraph-2k system (Oroboros Instruments, Innsbruck, Austria) (16). In brief, WAT was first mechanically permeabilized in respiratory medium (0.5 mM EGTA, 3 mM $MgCl_2$, 60 mM K-lactobionate, 10 mM KH_2PO_4, 20 mM HEPES, and 110 mM sucrose, pH 7.1) using a PBI-Shredder SG3 (Pressure BioScience, South Easton, MA, USA) in the presence of digitonin (8 μM). The equivalent of 80 mg wet tissue was added to the experimental chamber containing respiration media (described above), supplemented with 1 g/L fatty acid-free bovine serum albumin. $LEAK_L$ respiration was measured by the addition of NADH-linked substrates (complex I linked) malate (2 mM) and pyruvate (10 mM) in the absence of ADP [denoted as leak respiration in the absence of ADP and the presence of 2 mM malate and 10 mM pyruvate (PM_L) in figures]. Oxidative phosphorylation (oxphos) capacity, $OXPHOS_P$, was quantified by the addition of ADP (5 mM), followed by additions of glutamate (10 mM) for additional oxidation of reduced substrates through complex I [oxphos capacity in the presence of 5 mM ADP and 10 mM glutamate (PMG_P)] and succinate (complex II linked; 10 mM) for convergent electron flow through both NADH-linked and succinate-linked pathways [oxphos capacity in the presence of 5 mM ADP, 10 mM glutamate, and 10 mM succinate ($PMGS_P$)]. Subsequently, carbonylcyanide-4-(trifluoromethoxy)-phenylhydrazone (FCCP) was titrated to achieve maximum flux through the electron-transfer system (ETS_E; respiratory state determined in the presence of FCCP), fueled by the oxidation of substrates through complex CI and CII in the presence of 0.5 μM FCCP [($PMGS_E$); 0.5 μM]. Finally, we inhibited electron transport through complex I [maximum flux through the ETS fueled by the oxidation of substrates through CII in the presence of 0.5 μM FCCP (S_E)] and III by the sequential addition of rotenone (0.5 μM) and antimycin A (2.5 μM), respectively. The remaining oxygen flux after inhibition with antimycin A (O_2 flux independent of ETS) was subtracted from the values of each of the previous steps. Oxygen flux values were expressed relative to tissue wet weight per second (J_{O_2}, pmol O_2/mg/s).

Serological analysis

Serum was obtained from blood of PGC-1α/β-FAT-DKO mice (food withheld for 5h) and WT littermates either fed AL or subjected to CR. Insulin was assayed with an ultra-sensitive mouse insulin ELISA kit (Crystal Chem, Zaandam, The Netherlands). Free fatty acids were determined with the NEFA-C kit (Wako Chemicals, Neuss, Germany). Triglycerides and total cholesterol were measured using colorimetric commercial kits (FAR Diagnostics, Pescantina, Verona, Italy).

Glucose and insulin tolerance tests

Glucose tolerance tests (GTTs) and insulin tolerance tests (ITTs) were performed as detailed in Enguix *et al.* (10). For GTTs, mice first had food withheld for 12 h. After an intraperitoneal injection of 2 g/kg glucose, glycemia was determined at 0, 15, 30, 60, 90, and 120 min, using a Contour XT glucometer (Bayer, Leverkusen, Germany). ITTs were performed on mice that had food withheld for 5h and were injected with 0.9 U/kg insulin, and blood glucose levels were determined at the same time intervals specified for the GTT.

Analysis of insulin signaling

After withholding food overnight, mice were first anesthetized and then intravenously injected with 1 U/kg insulin. After 3 min, samples from WAT, liver, and skeletal muscle (gastrocnemius/soleus) were obtained, snap frozen, and stored at −80°C for subsequent analysis. Samples from the same tissues were obtained before the injection of insulin and were used as non-stimulated controls. Protein extracts from tissues were obtained in RIPA buffer (50 mM Tris, pH = 8.0, 150 mM NaCl, 1% Nonidet P-40, 0.5% sodium deoxycholate, 0.1% SDS) containing a protease and phosphatase inhibitor cocktail. Protein extracts (15–30 μg) were subjected to SDS-PAGE and immunoblotted with specific antibodies against total protein kinase B (AKT; 9272, 1:1000; Cell Signaling Technology), AKT phosphorylated at residue Thr308 (2965, 1:1000; Cell Signaling Technology), and CYPA (BML-SA296, 1:5000; Enzo Life Sciences).

Statistical analysis

Data are presented as means ± SEM. Statistical significance was assessed using an unpaired Student's *t* test or an ANOVA, followed by Tukey *post hoc* test.

RESULTS

Effects of CR on gene expression in WAT

To identify the main gene networks regulated by CR in WAT, we subjected mice to a 40% CR regime over a 12- wk period (**Fig. 1*A***). Whereas mice fed AL with a HF diet rapidly gained weight and became obese, CR mice fed the same diet remained lean throughout the experimental period (Fig. 1*B*). As expected, AL mice became glucose intolerant, whereas CR mice were protected from the deleterious effects of a HF diet on glucose metabolism (Fig. 1*C*).

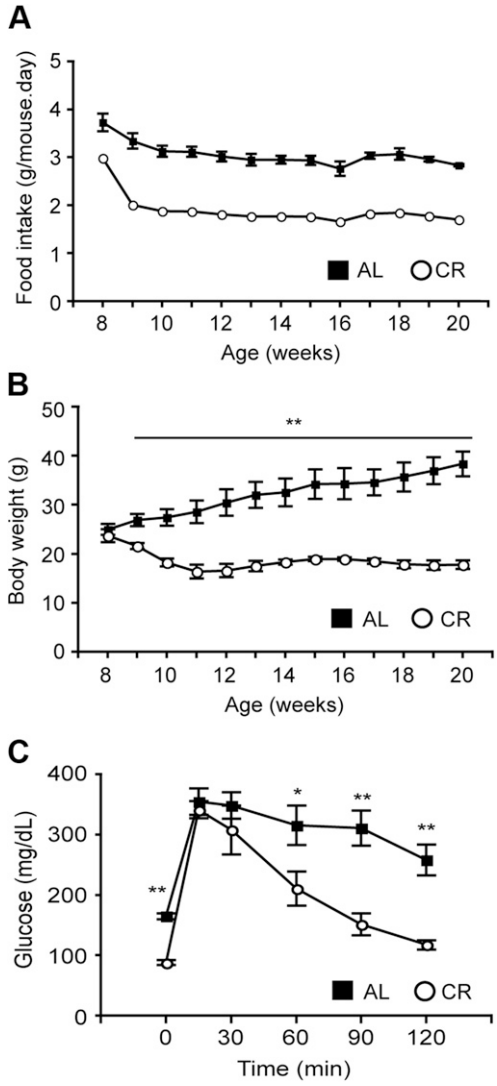

Figure 1. CR prevents the development of diet-induced obesity and glucose intolerance. At the age of 7 wk, individually caged WT C57BL6/J mice started receiving a HF diet (45% kcal from fat), and 1 wk later, they were randomly assigned to AL or CR groups. CR mice received 60% of the food eaten by AL animals for a period of 12 wk. *A*) Food intake of AL and CR mice. *B*) Body weight was measured weekly throughout the experimental period. *C*) GTTs (2 g/kg) were performed on AL and CR mice that had food withheld for 12 h. Results are expressed as means ± SEM (n = 10–12 animals/group). *$P < 0.05$, **$P < 0.01$.

To gain insight into the potential mechanisms and biologic pathways affected by CR in WAT, we conducted a gene-expression profiling study in inguinal WAT of AL and CR mice using DNA microarrays. We found 3740 genes differentially expressed in WAT of CR mice ($P < 0.05$), 1494 of which were upregulated and 2244 downregulated. Gene-enrichment analyses revealed that the gene network related to mitochondria was the most highly over-represented among the upregulated genes (**Fig. 2*A*** and **Table 1**). On the other hand, gene ontology (GO) categories related to extracellular matrix (ECM) were highly over-represented among the genes downregulated in WAT in response to CR (**Fig. 3*A***, left, and Table 1), although with lower statistical significance, we also found that GO categories related to the immune system (*i.e.*, inflammatory response, $P = 2.8E{-}9$; chemotaxis, $P = 9.4E{-}7$; wound healing, $P = 1.8E{-}5$) were significantly over-represented among the genes downregulated by CR (Fig. 3*B*, left).

qRT-PCR confirmed that mRNA expression of genes related to mitochondrial function, including genes of the oxphos system, the tricarboxylic acid cycle, and fatty acid oxidation, was highly increased in response to CR (Fig. 2*B*). The mRNA increase correlated with elevated levels of mitochondrial proteins (Fig. 2*C*). Such increase in the relative amount of mitochondrial proteins (mitochondrial protein content/protein unit of WAT) translates into a net increase in the absolute content of mitochondrial proteins in the inguinal WAT depot as a whole (mitochondrial protein content/WAT depot), despite the reduction in WAT mass imposed by CR (Supplemental Fig. S1*A*). Consequently, even if WAT mass is reduced in calorie-restricted mice, the increase in absolute mitochondrial protein content makes WAT a potential net contributor to oxidative metabolism in response to CR. Furthermore, we also found that CR increased mtDNA content by almost 3-fold (Fig. 2*D*), indicating that CR-induced mitochondrial gene expression was accompanied by an increase of mitochondrial mass in WAT. Moreover, CR also caused a severe reduction in the expression of genes encoding for structural proteins of the ECM, such as collagens, or genes involved in the remodeling of the ECM, such as metallopeptidases (Fig. 3*A*, right). Furthermore, a generalized decreased in the expression of genes related to the immune system was observed in WAT of calorie-restricted mice (Fig. 3*B*, right). These include both proinflammatory (*Il-6*, *Ccl2*, *Ccl7*) and anti-inflammatory genes (*Il-13*, *Il-33*), as well as markers of inflammatory M1 macrophages (*Cd11c*, *Nos2*) and anti-inflammatory M2 macrophages [*arginase 1* (*Arg1*)].

Increased mitochondrial mass and function have been proposed as main determinants of whole-body insulin sensitivity, but the role that mitochondria play

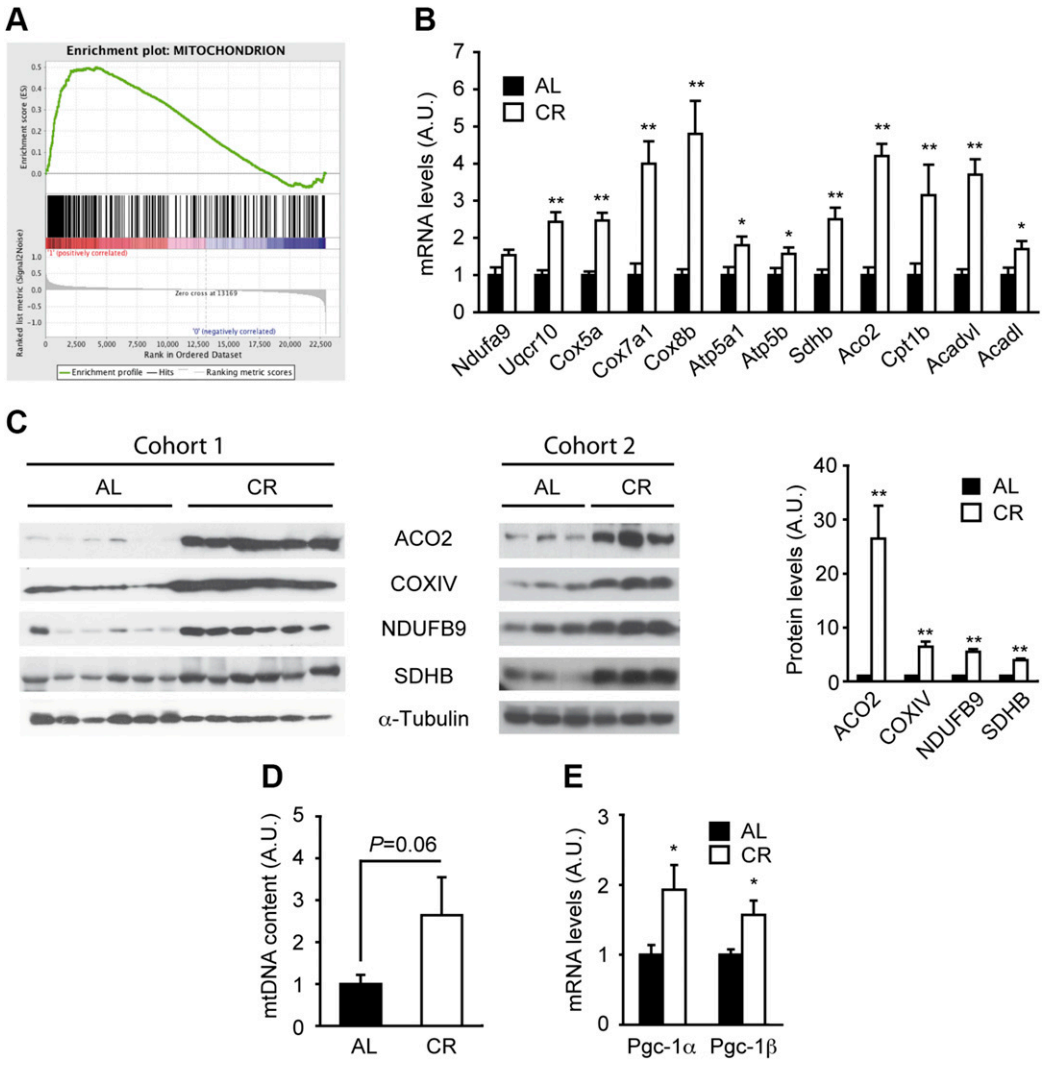

Figure 2. CR induces mitochondrial biogenesis in WAT. *A*) Gene-set enrichment analysis identified genes related to mitochondria as being differentially upregulated in inguinal WAT of WT mice subjected to 40% CR. *B*) mRNA expression of mitochondrial genes in inguinal WAT was assessed by qRT-PCR. *C*) Western blot of protein extracts from inguinal WAT of mice fed AL or subjected to 40% CR. The results obtained from 2 independent cohorts of mice are shown. Densitometric quantification of Western blots from the 2 cohorts of mice ($n = 9$ animals/group) is depicted (right). *D*) mtDNA content was assessed by qRT-PCR in total DNA isolated from inguinal WAT. *E*) mRNA levels of transcriptional coactivators PGC-1α and PGC-1β were assessed by qRT-PCR. Results are expressed as means ± SEM ($n = 5$–6 animals/group). *Acadl*, acyl-CoA dehydrogenase long chain; *Acadvl*, acyl-CoA dehydrogenase very long chain; *Cpt1b*, carnitine palmitoyltransferase 1B; *Uqcr10*, ubiquinol-cytochrome C reductase, complex III subunit X. $^*P < 0.05$, $^{**}P < 0.01$.

in the control of glucose homeostasis is still a matter of debate. For this reason, among other cellular processes regulated by CR, we decided to investigate the contribution of mitochondria to the metabolic effects of CR.

PGC-1 coactivators regulate CR-induced mitochondrial biogenesis in WAT

The coordinated induction of mitochondrial genes in response to CR was associated with an increase in the expression of PGC-1α and PGC-1β coactivators (Fig. 2*E*). Because PGC-1s appears to regulate mitochondrial biogenesis redundantly (17), we first aimed at investigating to which extent both types of PGC-1 are indeed required for the induction of mitochondrial biogenesis in response to CR. For this, we generated a new knockout mouse model simultaneously devoid of PGC-1α and PGC-1β in adipocytes (PGC-1α/β-FAT-DKO). The disruption of *Ppargc1a* and *Ppargc1b* genes resulted in an ~75–80% decrease in the expression of PGC-1α and PGC-1β mRNA in WAT and a >95% reduction in BAT (**Fig. 4*A***). PGC-1α/β-FAT-DKO mice exhibited a 30–50% reduction in the basal mRNA levels of mitochondrial genes in WAT (Fig. 4*B*) that correlated with reduced levels of mitochondrial proteins (Fig. 4*C*). We next examined by high-resolution respirometry how mitochondrial respiration in WAT was affected by the lack of PGC-1s (Fig. 4*D*). We found that adipose PGC-1α/β-FAT-DKO mitochondria exhibited a reduction in the electron flux through complex I (PMG_P) in the coupled state, when pyruvate/glutamate were used as

TABLE 1. *Gene-enrichment analysis of differentially expressed genes in WAT of mice subjected to 40% CR was performed using the DAVID Bioinformatics Database functional annotation tool*

Ontology	GO ID	GO term	Genes (*n*)	*P* (<1.0*E*−10)
Upregulated genes				
CC	GO:0005739	Mitochondrion	250	5.5E−102
CC	GO:0005743	Mitochondrial inner membrane	110	3.4E−72
BP	GO:0055114	Oxidation-reduction process	109	3.6E−43
BP	GO:0008152	Metabolic process	77	4.3E−31
MF	GO:0016491	Oxidoreductase activity	84	2.1E−28
BP	GO:0006629	Lipid metabolic process	73	3.3E−28
CC	GO:0070469	Respiratory chain	30	3.6E−28
BP	GO:0006631	Fatty acid metabolic process	42	2.9E−25
CC	GO:0005759	Mitochondrial matrix	40	7.4E−21
CC	GO:0005747	Mitochondrial respiratory chain complex I	22	1.9E−19
BP	GO:0006099	Tricarboxylic acid cycle	16	3.9E−15
MF	GO:0051287	NAD binding	17	2.2E−11
Downregulated genes				
CC	GO:007006	2 Extracellular exosome	343	4.4E−45
CC	GO:0031012	ECM	84	1.8E−33
CC	GO:0005578	Proteinaceous ECM	81	9.6E−29
CC	GO:0005576	Extracellular region	217	4.4E−25
CC	GO:0005615	Extracellular space	193	4.8E−24
BP	GO:0007155	Cell adhesion	88	1.6E−19
BP	GO:0001525	Angiogenesis	55	5.6E−17
MF	GO:0005515	Protein binding	366	4.3E−15
MF	GO:0008201	Heparin binding	39	7.1E−14
BP	GO:0030335	Positive regulation of cell migration	45	2.6E−13
MF	GO:0005178	Integrin binding	30	1.4E−12
MF	GO:0005509	Calcium ion binding	94	2.5E−12
MF	GO:0005518	Collagen binding	22	2.2E−11

BP, biologic process; CC, cellular component; MF, molecular function.

substrates in the presence of malate and ADP. Sequential addition of succinate allowed us to determine convergent electron flux through NADH- and succinate-linked pathways ($PMGS_P$), which was also impaired in WAT of PGC-1α/β-FAT-DKO mice. Likewise, maximum electron transport capacity with substrates fueling the ETS through ETS complexes CI and CII ($PMGS_E$) or only through CII after inhibiting CI with rotenone (S_E) was reduced in WAT of PGC-1α/β-FAT-DKO mice. Altogether, these results support a crucial role for PGC-1 coactivators in the maintenance of basal mitochondrial biogenesis and oxidative function in WAT.

Given the fact that CR-induced mitochondrial biogenesis was paralleled by an increase in the expression of PGC-1α and PGC-1β, we next investigated whether simultaneous lack of both coactivators could affect the process of mitochondrial biogenesis in response to CR. For this, WT and PGC-1α/β-FAT-DKO mice were either fed AL with a HF diet or subjected to a 40% CR for 12 wk. PGC-1α and PGC-1β expression was confirmed to increase in WAT of WT mice in response to CR (**Fig. 5*A***) and correlated with an increase in the expression of mitochondrial genes, both at the mRNA and protein levels (Fig. 5*B, C* and Supplemental Fig. S1*B*). However, enhanced mitochondrial gene expression in response to CR was severely blunted in WAT of PGC-1α/β-FAT-DKO mice (Fig. 5*B, C* and Supplemental Fig. S1*B*). Likewise, the increase in mtDNA content on CR was impaired in mice lacking PGC-1 coactivators (Fig. 5*D*). In addition, we found that CR enhanced WAT oxidative function in WT mice, an effect that was impaired in PGC-1α/β-FAT-DKO mice (Fig. 5*E*).

Basal mitochondrial biogenesis and *Ucp1* expression are regulated by PGC-1 coactivators in BAT but not by CR

Consistent with the well-known role of PGC-1 coactivators in the thermogenic function of brown adipocytes (18), BAT of PGC-1α/β-FAT-DKO mice showed an increase in the accumulation of triglycerides, a clear indication of poor thermogenic activity (**Fig. 6*A***). As expected, lack of PGC-1 coactivators in brown adipocytes resulted in a severe decrease in the expression of genes encoding for mitochondrial proteins, including *Ucp1* (Fig. 6*B*). The expression levels of mRNA correlated with lower levels of mitochondrial proteins (Fig. 6*C*). However, unlike in WAT, we did not observed any induction by CR of the expression of genes encoding for PGC-1α, PGC-1β, or mitochondrial genes, with the exception of *CoxIV*, in which its expression was found to be mildly but significantly increased in response to food deprivation (Fig. 6*D*). Furthermore, *Ucp1* mRNA levels were not affected by CR, although its basal expression was entirely dependent on PGC-1 coactivators. Similar findings were observed at the protein levels, with mitochondrial proteins, including UCP1, not being affected or even mildly reduced by CR (Fig. 6*E* and

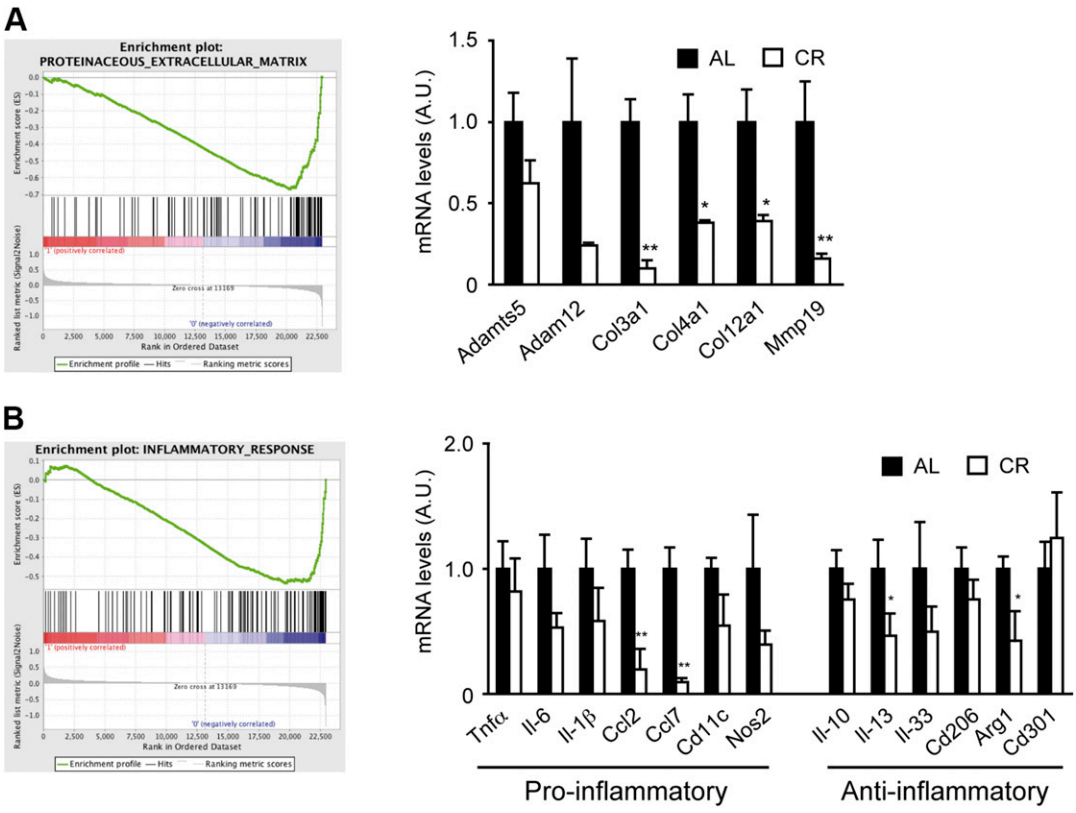

Figure 3. CR reduces the expression of genes related to ECM remodeling and inflammation. Genes related to ECM (*A*) and the inflammatory response (*B*) were found to be downregulated in WAT of mice subjected to CR. Gene expression was validated by qRT-PCR. Results are expressed as means ± SEM (n = 5–6 animals/group). *Adam12*, ADAM metallopeptidase domain 12; *Adamts5*, ADAM metallopeptidase with thrombospondin type 1 motif 5; *Col*, collagen; *Mmp19*, matrix metalloproteinase 19. $*P < 0.05$, $**P < 0.01$.

Supplemental Fig. S2). Altogether, these data suggest that basal mitochondrial biogenesis in BAT is highly dependent on PGC-1 coactivators but that brown adipocyte mitochondrial gene expression and thermogenic activity are not enhanced by CR, contrary to what we observed in WAT.

CR does not induce browning of WAT

It has been recently reported that CR induces the recruitment of brown adipocytes within WAT depots. It has also been suggested that such a browning process could contribute to the positive effects that CR has on glucose homeostasis (19). In WT mice, despite careful examination of histologic preparations of WAT, no cells with the characteristic morphology of brown adipocytes were found in mice subjected to CR (**Fig. 7*A***). Nevertheless, at the molecular level, a very modest and variable increase in the *Ucp1* and cell death-inducing DNA fragmentation factor α-like effector A (*Cidea*) but not PR domain zinc finger protein 16 (*Prdm16*) mRNA levels was observed in WAT of CR mice (Fig. 7*B*). The mild induction of *Ucp1* and *Cidea* mRNA was completely blunted in PGC-1α/β-FAT-DKO mice (Fig. 7*C*). Importantly, despite the moderate increase in mRNA levels, we were unable to detect UCP1 protein in WAT of WT and PGC-1α/β-FAT-DKO mice, irrespective of the nutritional treatment (Fig. 7*D*), indicating that detectable browning of WAT does not occur in response to CR.

CR-induced mitochondrial biogenesis is not required for the improvement in glucose homeostasis exerted by CR

Increased mitochondrial biogenesis in WAT has been suggested to be instrumental in the amelioration of insulin resistance by certain pharmacological or lifestyle interventions [reviewed in Zamora and Villena (8)]. The dramatic induction of mitochondrial biogenesis in response to CR suggests that enhanced mitochondrial oxidative function in WAT could be required by CR to exert its beneficial effects on glucose homeostasis.

PGC-1α/β-FAT-DKO mice did not exhibit differences in body weight when either fed a regular chow diet (data not shown) or a HF diet (**Fig. 8*A***), neither did they show differences in the weight of major organs, including different depots of WAT, BAT, liver, and gastrocnemius muscle (Fig. 8*B*). In WT and PGC-1α/β-FAT-DKO mice, CR intervention similarly reduced the weight of BAT, liver, and all depots of WAT with the exception of epididymal WAT, which remained almost unaffected by CR (Fig. 8*B*). No differences were found in the gastrocnemius muscle, indicating that lean mass was not affected by the lack of PGC-1s or by the nutritional intervention.

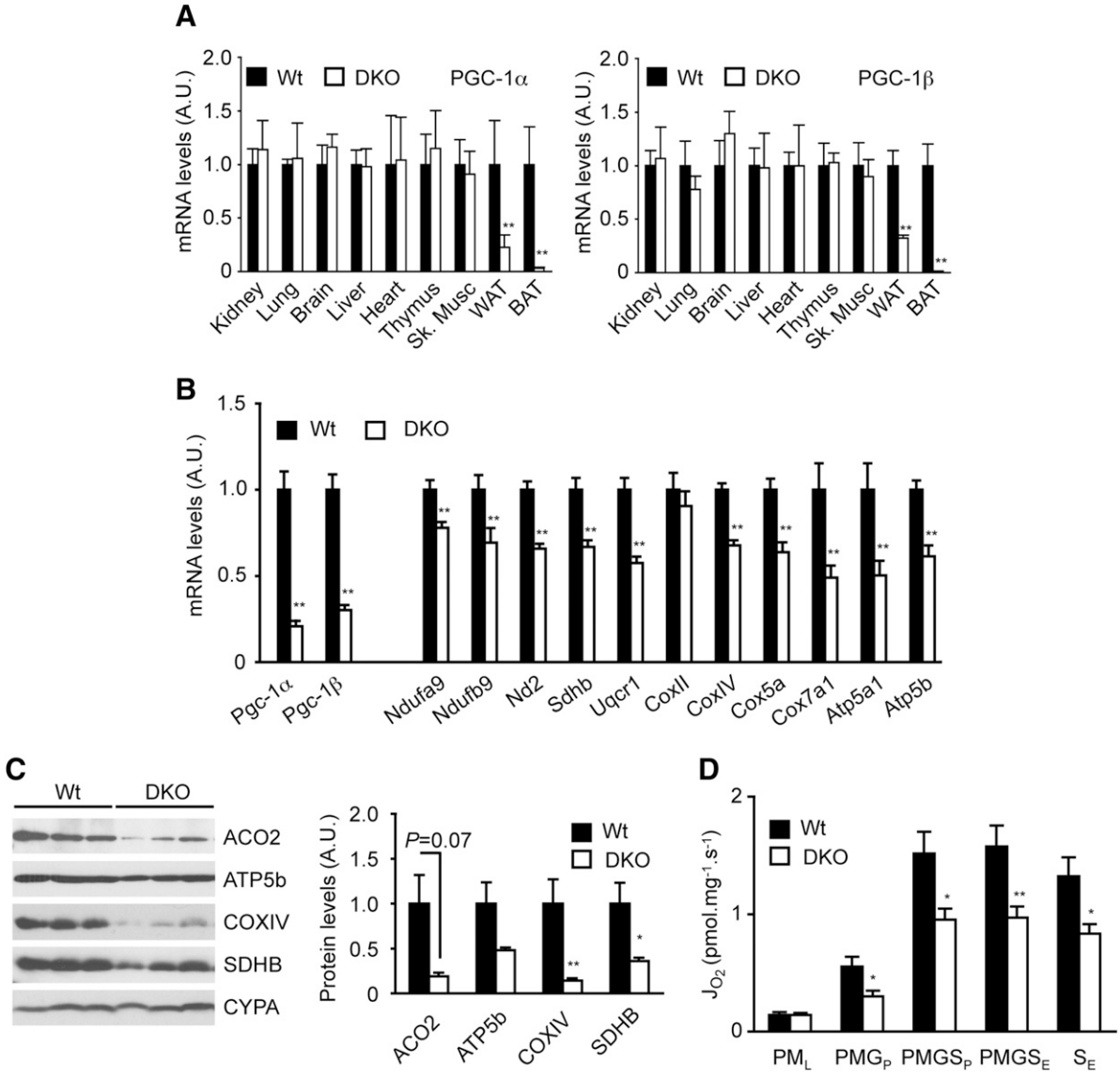

Figure 4. Adipose-specific lack of PGC-1α and PGC-1β coactivators leads to reduced mitochondrial gene expression and reduced mitochondrial respiration in WAT. *A*) mRNA expression of PGC-1α (left) and PGC-1β (right) in tissues of WT and PGC-1α/β-FAT-DKO mice was analyzed by qRT-PCR ($n = 4$–5 animals/group). *B*) Mitochondrial gene expression in inguinal WAT of WT and PGC-1α/β-FAT-DKO mice analyzed by qRT-PCR (n = 10–12 animals/group). *C*) Western blots of mitochondrial proteins in inguinal WAT of WT and PGC-1α/β-FAT-DKO mice (left). Densitometric quantification of blots (right). *D*) Mitochondrial respiration in inguinal WAT was assessed by high-resolution respirometry (PM_L, PMG_P, $PMGS_P$, $PMGS_E$, and S_E). Results are expressed as means ± SEM (n = 5 animals/group). JO_2, oxygen flux value; *Nd2*, NADH dehydrogenase subunit 2. $^*P < 0.05$, $^{**}P < 0.01$.

AL feeding with a HF diet induced severe glucose intolerance and insulin resistance in both WT and PGC-1α/β-FAT-DKO mice (**Fig. 9*A, D***). Although it has been speculated that impaired WAT mitochondrial function could lead to the development of insulin resistance, we did not observe significant differences in insulin sensitivity between WT and PGC-1α/β-FAT-DKO mice fed AL when an ITT was performed (Fig. 9*D, F*). Likewise, no significant differences were found between WT and PGC-1α/β-FAT-DKO mice fed AL in their capacity to clear glucose from circulation during an intraperitoneal GTT (Fig. 9*A, C*). When subjected to CR, both WT and PGC-1α/β-FAT-DKO mice improved whole-body glucose tolerance and insulin sensitivity to the same extent (Fig. 9*A*–*F*). Consistent with a healthier metabolic status, both WT and PGC-1α/β-FAT-DKO mice exhibited a similar reduction in fasting glucose, insulin, and lipid levels when subjected to CR (**Table 2**).

Although whole-body glucose homeostasis did not appear altered in PGC-1α/β-FAT-DKO mice, it is possible that impaired mitochondrial function in adipocytes could lead to adipose tissue-specific insulin resistance. However, as shown in Fig. 9*G*, insulin administration led to a similar increase in AKT phosphorylation in WAT of both WT and PGC-1α/β-FAT-DKO mice, indicating that impaired mitochondrial biogenesis and oxidative function do not impair insulin signaling in WAT. Moreover, in agreement with the general improvement in insulin sensitivity

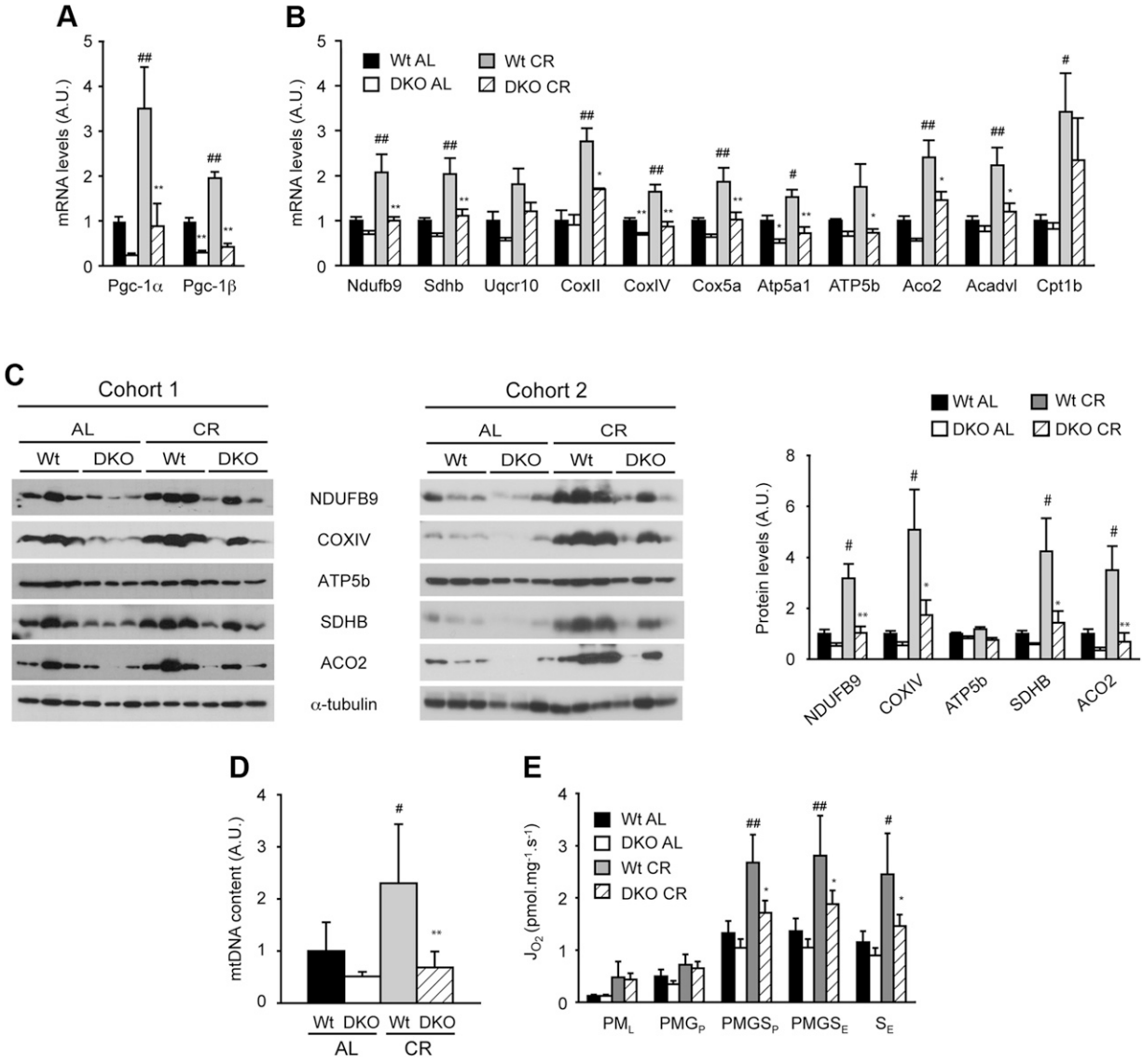

Figure 5. CR-induced mitochondrial biogenesis in WAT is dependent of PGC-1 coactivators. *A*, *B*) mRNA expression of PGC-1α and PGC-1β coactivators (*A*) and genes encoding for mitochondrial proteins (*B*) in WAT of WT and PGC-1α/β-FAT-DKO mice fed AL or subjected to CR were analyzed by qRT-PCR (n = 10–12 animas/group). *C*) Western blots of mitochondrial proteins in inguinal WAT from 2 independent cohorts of mice. Densitometric analysis of blots from the 2 cohorts of mice is shown in the graph. *D*) mtDNA content in WAT. *E*) Mitochondrial function in inguinal WAT of AL and CR mice was assessed by high-resolution respirometry (PM_L, PMG_P, $PMGS_P$, $PMGS_E$, and S_E). Results are expressed as means ± SEM (n = 6–8 animals/group). $^*P < 0.05$, WT *vs.* PGC-1α/β-FAT-DKO mice; $^{\#}P < 0.05$, AL *vs.* CR; $^{**}P < 0.01$ WT *vs.* PGC-1α/β-FAT-DKO mice; $^{\#\#}P < 0.01$, AL *vs.* CR.

observed, CR notably improved insulin-stimulated AKT phosphorylation in WAT of WT animals. Despite the inability of PGC-1α/β-FAT-DKO mice to increase mitochondrial mass and oxidative function in response to CR, WAT of mice lacking PGC-1 coactivators normally respond to insulin stimulation by increasing AKT phosphorylation to the same extent as WT. Similar results were obtained in liver and skeletal muscle (Fig. 9*G*).

DISCUSSION

CR is well known for having positive effects on glucose homeostasis, improving whole-body insulin sensitivity, and enhancing insulin-dependent glucose uptake in skeletal muscle, liver, and WAT (20, 21). Still, the precise mechanisms by which CR improves diet-induced insulin resistance have not been defined.

Several studies in rodents and humans have reported an increase in mitochondrial gene expression in both human and rodent tissues (22–25). However, the effect of CR on mitochondrial biogenesis has remained controversial, and other studies have reported the lack of any change in mitochondrial protein content induced by low-caloric regimes (26). Our gene-expression profiling study reveals that CR dramatically enhances the expression of genes related to oxidative metabolism and promotes mitochondrial biogenesis in mouse WAT, joining ranks with other

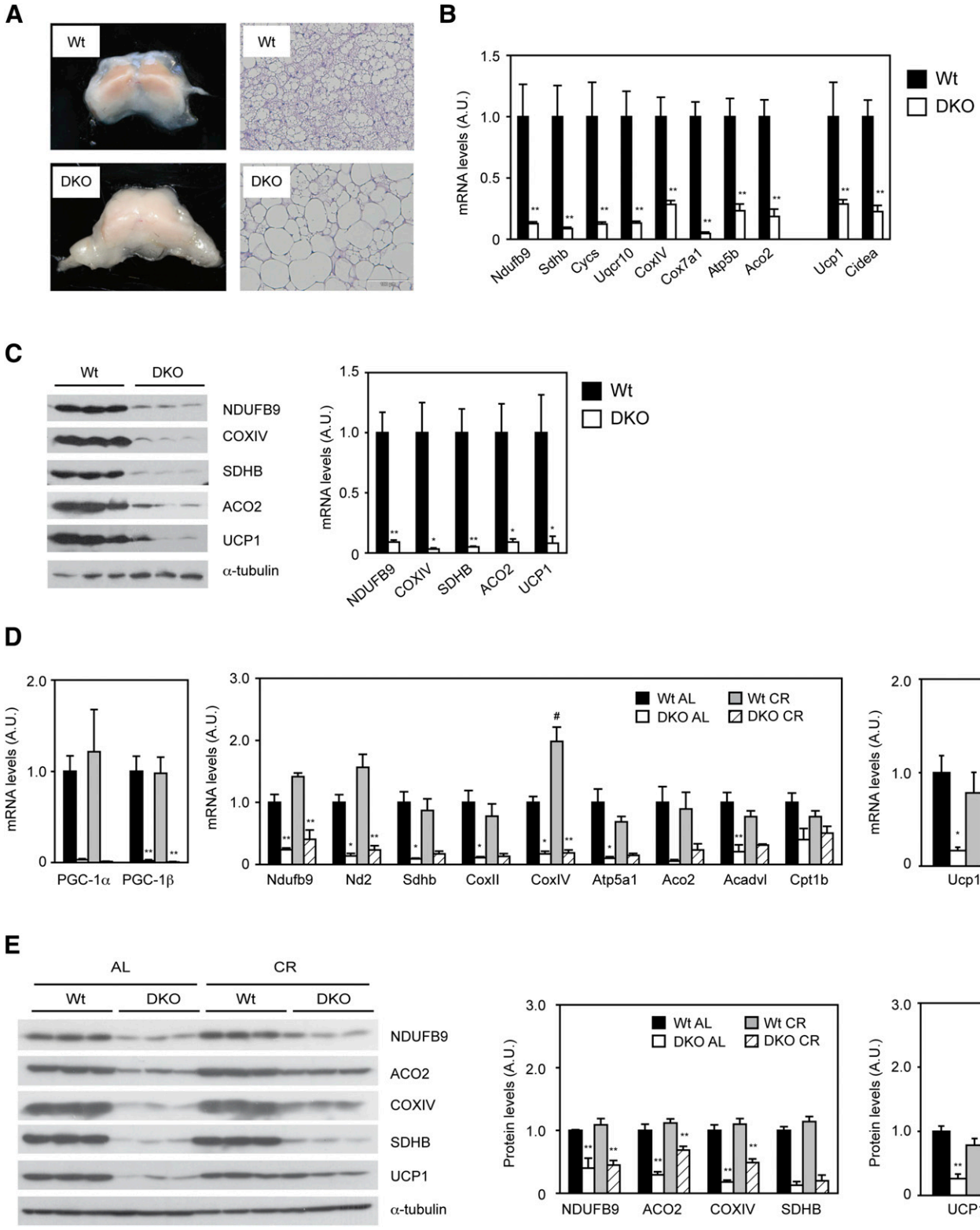

Figure 6. PGC-1 coactivators but not CR regulate mitochondrial biogenesis in BAT. *A*) Gross morphologic aspect of interscapular BAT of PGC-1α/β-FAT-DKO mice and WT littermates (left). Histologic sections of BAT were stained with hematoxylin/eosin (right). *B*) Expression of mitochondrial genes in interscapular BAT of WT and PGC-1α/β-FAT-DKO mice ($n = 6$ animals/group) was assessed by qRT-PCR. *C*) Western blots of mitochondrial proteins in BAT of WT and PGC-1α/β-FAT-DKO mice (left). Densitometric quantification of blots (right). *D*) mRNA expression of PGC-1α and PGC-1β coactivators and genes encoding for mitochondrial proteins, including *Ucp1*, in BAT of WT and PGC-1α/β-FAT-DKO mice fed AL or subjected to CR was analyzed by qRT-PCR ($n = 4$ animas/group). *E*) Western blots of mitochondrial proteins in BAT of WT and PGC-1αβ-FAT-DKO mice fed AL or subjected to CR (left). Densitometric analysis of blots is shown (right). Results are expressed as means ± SEM. $^{*}P < 0.05$, WT *vs.* PGC-1α/β-FAT-DKO mice; $^{\#}P < 0.05$, AL *vs.* CR; $^{**}P < 0.01$. *Cycs*, cytochrome C, somatic.

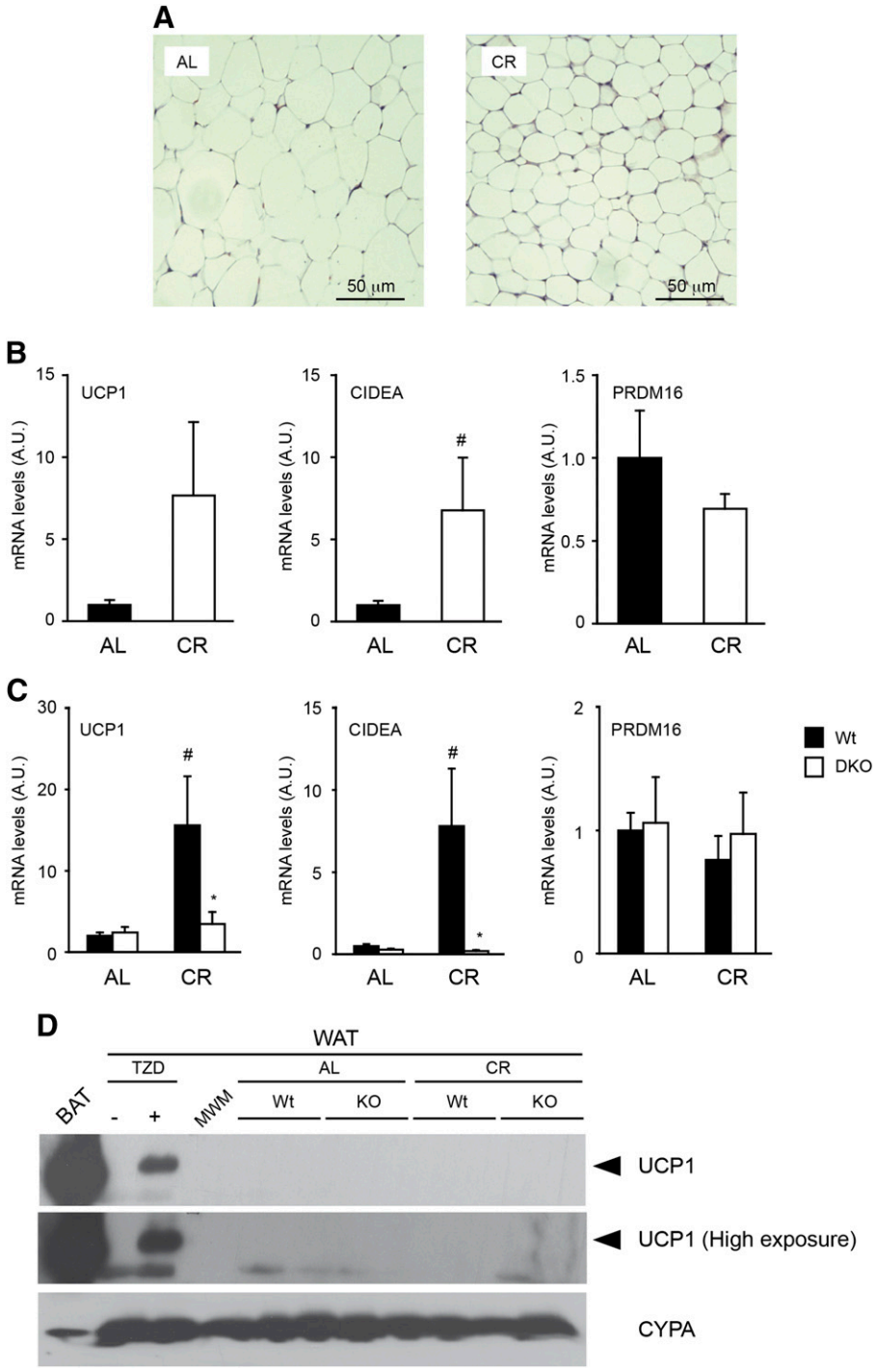

Figure 7. Analysis of the PGC-1-dependent browning of WAT in response to CR. *A*) Hematoxylin/eosin-stained histologic sections of inguinal WAT from AL and CR mice. *B*) mRNA expression of brown adipocyte markers in inguinal WAT from AL and CR mice was assessed by qRT-PCR. *C*) mRNA expression of brown adipocyte markers in inguinal WAT of WT and PGC-1α/β-FAT-DKO mice, either fed AL or subjected to CR assessed by qRT-PCR. *D*) Western blot of UCP1 in protein extracts of inguinal WAT from WT and PGC-1α/β-FAT-DKO mice fed AL or subjected to CR. Five micrograms of protein extracts from BAT was used as positive control for UCP1. Fifty micrograms of protein extracts from WAT of WT mice treated with 10 mg/kg rosiglitazone for 10 d was used as a positive control of WAT browning. Results are expressed as means ± SEM (n = 6–7 animals/group). $^{*}P < 0.05$, WT *vs.* PGC-1α/β-FAT-DKO mice; $^{\#}P < 0.05$, AL *vs.* CR. MWM, MW marker. *Prdm16*, PR domain zinc finger protein 16.

studies to support a positive effect of CR on mitochondrial metabolism. The coordinated increase in mitochondrial gene expression appears as a common signature of CR in many tissues, but its physiologic implications with regard to the health benefits exerted by CR had not been adequately addressed before. In this study, we show that CR-induced mitochondrial biogenesis in WAT depends on the transcriptional activity of PGC-1 coactivators, unequivocally demonstrating that PGC-1 acts as a master regulator of mitochondrial biogenesis (17), also in response to low-calorie intake. Several studies had pointed toward PGC-1α as a major regulator of mitochondrial biogenesis induced by CR based on the observation that PGC-1α mRNA levels are increased in rodents and humans subjected to mid- or long-term CR (23, 25, 27). However, only a recent study has provided experimental evidence that supports the involvement of PGC-1α in the regulation of mitochondrial genes during CR in skeletal muscle. In that study, with the use of muscle-specific PGC-1α knockout mice, Finley *et al.* (28) demonstrated that the mitochondriogenic response observed in skeletal muscle upon CR was blunted in the absence of PGC-1α. In our study, the use of a mouse model simultaneously devoid of PGC-1α and PGC-1β in adipocytes does not allow

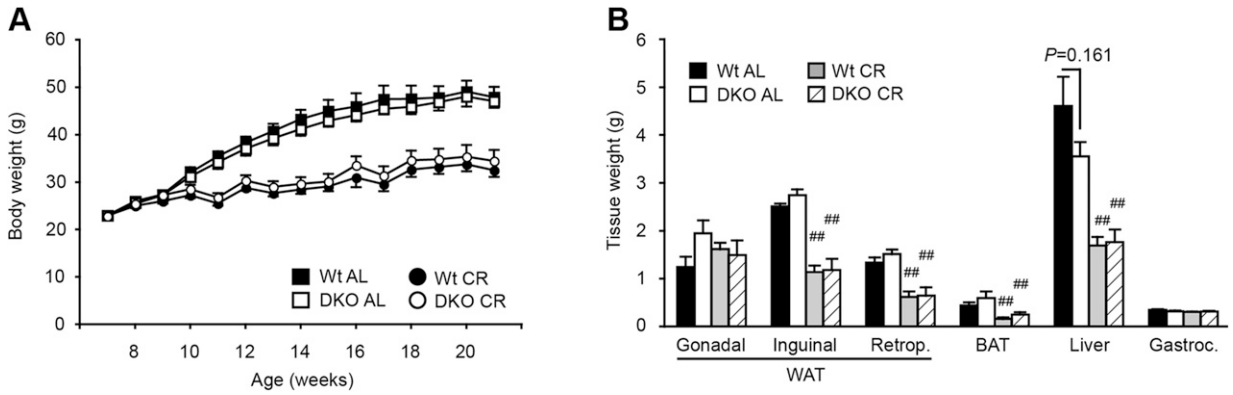

Figure 8. Lack of PGC-1 coactivators does not alter body weight or adiposity. Body (*A*) and tissue (*B*) weight of WT and PGC-1α/β-FAT-DKO mice, either fed AL or subjected to CR for 12 wk. All animals were fed the same HF diet (45% kcal fat, 35% kcal carbohydrates, 20% kcal protein). Results are expressed as means ± SEM (n = 5–6 animals/group). $^{\#\#}P < 0.01$, AL *vs.* CR.

discrimination of which one of the two coactivators acts as the main driver of mitochondrial gene expression in response to CR in WAT. Still, in white adipocytes, a cooperative contribution between PGC-1α and PGC-1β to the control of mitochondrial gene expression in response to CR is very likely. Indeed, first, both PGC-1α and PGC-1β mRNA levels are induced in WAT in response to CR; second, we have previously shown that PGC-1β appears to have a dominant role over PGC-1α in the regulation of mitochondrial gene expression in white adipocytes (10, 11); and third, contrary to what it was previously assumed, PGC-1β also plays an important role in the dynamic regulation of mitochondrial gene expression in response to cues that prompt for increased mitochondrial oxidative function [*i.e.*, thiazolidinediones (TZDs)] beyond its well-known role in the maintenance of basal mitochondrial mass (10).

Our study provides experimental evidence that places PGC-1 coactivators as central elements that integrate the input of different regulatory signals to modulate mitochondrial biogenesis in response to CR. Such signals activated by nutrient/energy deprivation include Sirtuin 1 (Sirt1), a NAD^+-dependent deacetylase; AMPK, an AMP/ADP-activated kinase; and eNOS, all of which are activated by CR. Thus, increase in the deacetylation (29, 30) and phosphorylation (31) by Sirt1 and AMPK, respectively, would lead to the transcriptional activation of PGC-1s, whereas increased NO production by eNOS would enhance the expression of, at least, PGC-1α (25). The integration of all of these regulatory signals would result in a net boost of PGC-1 coactivators transcriptional activity and the consequent increase in mitochondrial biogenesis in response to CR.

Numerous studies have shown the existence of a tight correlation between insulin sensitivity and mitochondrial mass/oxidative function in skeletal muscle and WAT [reviewed in Zamora and Villena (8)]. Consequently, mitochondrial oxidative capacity has been considered a strong predictor of insulin sensitivity (32). In this regard, it is worth noting that several therapeutic interventions that improve glucose homeostasis are associated with increased mitochondrial biogenesis and oxidative function in WAT. For example, TZDs, a family of anti-diabetic drugs, have been shown to induce mitochondrial biogenesis, specifically in WAT of genetically and diet-induced insulin resistance and T2D animal models (33, 34), as well as in humans (35, 36), concomitantly with an improvement in insulin sensitivity. Likewise, treatment of rodent models with resveratrol or selective synthetic activators of Sirt1 has been reported to improve insulin resistance in close association with an increase in mitochondrial biogenesis and function in WAT, skeletal muscle, and liver (37, 38). Based on this tight association, it has been suggested that the increase of mitochondrial mass in WAT and/or other tissues would be one of the major mechanisms by which CR contributes to the reversal of insulin resistance. However, our data, showing that mice lacking PGC-1 coactivators fail to increase adipose mitochondrial biogenesis but still retain their full capacity to improve whole-body glucose tolerance and insulin sensitivity in response to CR, strongly support the notion that enhanced mitochondrial function in adipocytes is not absolutely required for the positive effects that CR exerts on glucose homeostasis. These findings are in line with a previous study in which by using a mouse model with partial deficiency in mitochondrial function as a result of the adipose-specific deletion of PGC-1β, we demonstrated that rosiglitazone-induced mitochondrial oxidative capacity in WAT was not essential for the insulin-sensitizing effects of TZDs (10).

The adipose-specific nature of our PGC-1α/β-FAT-DKO mouse model raises the question of whether CR could improve whole-body glucose homeostasis by enhancing mitochondrial function in insulin target tissues other than WAT. Although this appears plausible, a study in muscle-specific PGC-1α knockout mice demonstrated that despite failure to increase mitochondrial mass and oxidative metabolism in skeletal muscle, muscle-specific PGC-1α knockout mice responded to CR by improving glucose tolerance and insulin sensitivity to the same extent as their WT counterparts (28). This is similar to what we described here for PGC-1α/β-FAT-DKO mice in WAT. Therefore, besides being a distinctive signature of CR in many tissues, altogether, these studies demonstrate a clear dissociation between CR-induced mitochondrial

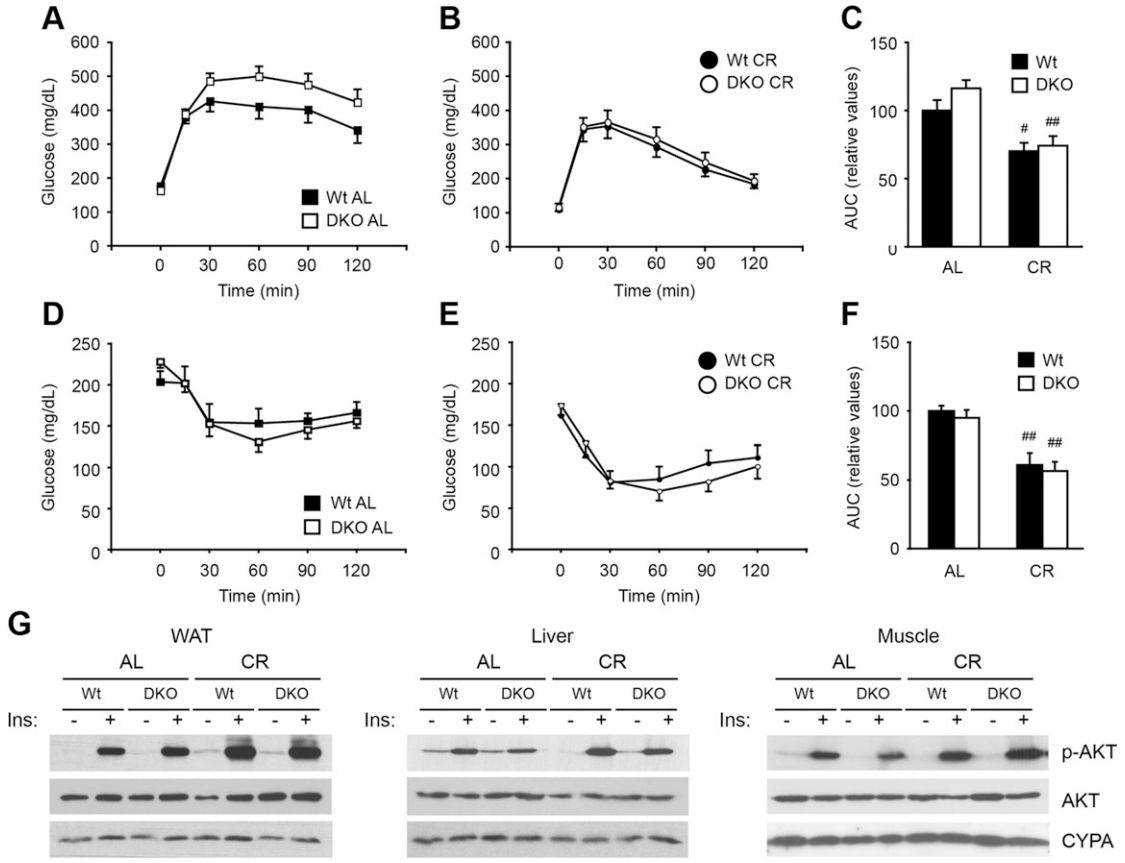

Figure 9. Impaired mitochondrial biogenesis in mice devoid of PGC-1 in adipose tissues does not prevent the amelioration of glucose homeostasis in response to CR. *A*, *B*) GTTs (2 g/kg) in WT and PGC-1α/β-FAT-DKO mice, either fed AL (*A*) or subjected to CR (*B*). *C*) Area under the curve (AUC) of GTTs. *D*, *E*) ITTs (0.9 U/kg) in WT and PGC-1α/β-FAT-DKO mice, either fed AL (*D*) or subjected to CR (*E*) for 12 wk. *F*) Area under the curve of ITTs. *G*) Tissue-specific insulin signaling. Total and phosphorylated (p-) Akt was detected by Western blot in protein lysates of inguinal WAT, liver, and gastrocnemius muscle from WT and PGC-1α/β-FAT-DKO mice, either fed AL or subjected to CR, which were treated with an insulin bolus after having food withheld for 12 h. CYPA was used as loading control. Results are expressed as means ± SEM (n = 5–6 animals/group). $^{\#}P \leq 0.05$, $^{\#\#}P \leq 0.01$, AL *vs.* CR.

biogenesis in WAT/muscle and the beneficial effects that this nutritional intervention exerts on glucose homeostasis.

If the induction of mitochondrial biogenesis and oxidative function in WAT and muscle are not required to ameliorate diet-induced insulin resistance in response to CR, then the question is by which other means CR exerts its beneficial effects on glucose homeostasis? Very recently, it has been reported that CR induces browning of WAT, an effect that appears to be mediated by an enhancement of type 2 immune response (19) and that has been associated with metabolic improvement during CR. Consistent with this observation, we were able to observe a moderate increase in the mRNA levels of brown adipocyte markers, such as *Ucp1* and *Cidea*, in response to CR. However, despite the changes observed in mRNA, the failure to find brown-like adipocytes and detectable levels of UCP1 protein within WAT of CR mice rather suggest that the browning of WAT in response to CR is negligible and irrelevant from a thermogenic point of view (39). Our data are further supported by a recent study in obese humans that also reported the absence of browning in response to CR (40). The lack of significant browning induced by CR contrasts with the tangible browning capacity of other agents, such as TZDs, which we showed were capable of inducing detectable levels of UCP1 in WAT (9, 10). Moreover, induction of UCP1 mRNA in WAT in response to CR appears blunted in PGC-1α/β-FAT-DKO mice, in agreement with the relevant role of PGC-1 coactivators in brown adipocyte differentiation and function (18). Still, PGC-1α/β-FAT-DKO mice improve glucose homeostasis in response to nutrient deprivation to the same extent as WT mice. Therefore, regardless of the magnitude of the browning induced by CR, our results strongly support the notion that brown adipocyte recruitment in WAT is not required for the effects of CR on glucose homeostasis.

It is also well known that PGC-1 coactivators are required for proper BAT function, controlling mitochondrial biogenesis during the course of adipocyte differentiation and the expression of the thermogenic program in response to low environmental temperatures (17). In agreement with the crucial role of PGC-1 coactivators in BAT, our PGC-1α/β-FAT-DKO mice exhibit a severe reduction in the levels of mitochondrial proteins and UCP1 in BAT that leads to a massive accumulation of triglycerides within brown adipocytes as a result of their incapacity to oxidize fatty acids properly into mitochondria and perform thermogenesis. Although reduced BAT mass and

TABLE 2. *Serological parameters in WT and PGC-1α/β-FAT-DKO mice fed AL with a HF diet or subjected to 40% CR for 12 wk*

	AL		CR	
Parameter	WT	PGC-1α/β-FAT-DKO	WT	PGC-1α/β-FAT-DKO
Glucose, mg/dl	203.5 ± 6.4	222.2 ± 11.5	161.3 ± 14.4*	173.8 ± 11.8*
Triglycerides, mg/dl	55.17 ± 3.37	49.42 ± 3.02	45.42 ± 2.69†	44.05 ± 2.33
Free fatty acids, mM	0.71 ± 0.06	0.73 ± 0.09	0.62 ± 0.08	0.59 ± 0.05
Cholesterol, mg/dl	267.7 ± 19.1	224.2 ± 19.6	174.1 ± 10.4*	154.7 ± 9.4*
Insulin, ng/ml	4.88 ± 0.45	3.45 ± 0.28‡	1.80 ± 0.22*	1.25 ± 0.12*

Data are expressed as means ± SEM. †$P \leq 0.05$, AL *vs.* CR; ‡$P \leq 0.05$, WT *vs.* PGC-1α/β-FAT-DKO mice; *$P \leq 0.01$.

impaired thermogenic activity have been correlated with higher body weight and impaired insulin sensitivity in rodents and humans (41–43), our results show that dysfunctional BAT in mice lacking PGC-1 coactivators is not sufficient to bring about an obese or insulin-resistant phenotype. Importantly, contrary to what we observed in WAT, CR does not induce mitochondrial biogenesis in BAT nor does it increase UCP1 expression, suggesting that CR does not activate brown adipocyte thermogenesis. The lack of response of UCP1 expression to CR is consistent with other studies reporting that UCP1 content or activity in BAT is unchanged (44) or even reduced (19, 45) in rodent models subjected to long-term, low-calorie intake, an effect that appears to be intended to increase calorie efficiency and maintain energy balance. The lack of induction of mitochondrial biogenesis and UCP1 protein levels in BAT in response to CR, strongly suggests that BAT does not play a relevant role in mediating the metabolic effects of CR.

Our study identified genes related to ECM remodeling and the immune system, as 2 gene networks significantly downregulated by CR in WAT. The microenvironment provided by ECM proteins is essential for proper development and function of adipose tissue, as ECM remodeling is fundamental for WAT to adapt to changing nutritional conditions (46). Thus, whereas ECM proteins are required for proper differentiation of precursors cells into fully functional adipocytes, excessive deposition of ECM proteins (*i.e.*, fibrosis) restrains migration of precursor cells and adipocyte hypertrophy, compromising adipose tissue expandability. Regarding the potential role of ECM in metabolic diseases, it has been shown that increased expression in WAT of ECM genes, including collagen (*COL*)*6A3* and matrix metalloproteinase 9, associates with increased body mass and tissue inflammation in humans (47, 48), 2 major risk factors for the development of insulin resistance and T2D. Consistent with an important role of adipose ECM in determining insulin sensitivity, mice that overexpress endotrophin, a cleavage product of COL6A3, develop WAT fibrosis and exhibit insulin resistance when fed a HF diet, an effect that is reversed after endotrophin neutralization (49). Likewise, obese COL6A3 knockout mice show an improvement in insulin sensitivity (50). Based on the positive effects that the reduction of ECM in WAT has on whole-body glucose homeostasis, it is plausible to speculate that CR may improve insulin resistance, at least in part, by downregulating the expression of genes encoding for ECM proteins and reducing fibrosis.

The anti-inflammatory effect of CR in WAT could also be an important contributor to the improvement of glucose homeostasis. It is well known that obesity-linked insulin resistance is associated with low-degree chronic inflammation of WAT, which is characterized by increased recruitment of M1 macrophages and other immune cells, elevated levels of proinflammatory cytokines, and the activation of NF-κB and JNK pathways that directly inhibit insulin signaling (51). The reduction in the expression of inflammatory cytokines (*i.e.*, *Il-1β* and *Il-6*) or chemokines (*i.e.*, *Ccl2* and *Ccl7*), together with the decrease, albeit not significant, in the levels of M1 proinflammatory macrophage markers (*Cd11c* and *Nos2*) that we observed in WAT of mice subjected to CR is in line with other studies demonstrating that CR reduces WAT inflammation in rodents (52, 53) and humans (54). Recent evidence suggests that CR enhances polarization of macrophages toward the alternative M2 anti-inflammatory phenotype (19), a switch that appears to contribute significantly to the improvement of insulin sensitivity (55). Contrary to what has been reported by Fabbiano *et al.* (19), the expression of anti-inflammatory cytokines (*i.e.*, *Il-13* and *Il-33*) and M2 markers (*i.e.*, *Arg1*) was reduced by CR in our study. This argues against an enhancement of macrophage polarization by CR, but it certainly indicates that reduced calorie intake decreases macrophage recruitment induced by HF feeding in WAT. The discrepancy between our study and the one from Fabbiano et al. (19) is unclear, but the different dietary regime (HF diet *vs.* regular chow) could have contributed to the different outcomes regarding not only macrophage polarization but also browning of WAT. Nevertheless, the evidences provided on the immune response to CR suggest that attenuation of diet-induced inflammation in WAT could contribute to the improvement of glucose homeostasis in response to CR.

In summary, our study has identified mitochondrial biogenesis as the main process positively regulated by CR in WAT. With the use of a new mouse model that simultaneously lacks the expression of PGC-1α and PGC-1β coactivators specifically in adipocytes, we have demonstrated that PGC-1 coactivators control the process of mitochondrial biogenesis in WAT in response to CR. Furthermore, we have shown that the induction of mitochondrial biogenesis and enhancement of mitochondrial oxidative function in WAT are not required for the positive

effects that CR exerts on glucose homeostasis. These findings support the notion that mitochondrial function in WAT is dissociated from insulin sensitivity, both under basal conditions and in response to CR. The mechanisms by which CR improves adipose and whole-body insulin sensitivity still remain to be defined, but our findings that pathways related to ECM and the immune response are also modulated by CR would deserve further exploration to unveil their relevance in the metabolic effects exerted by low-calorie intake. FJ

ACKNOWLEDGMENTS

The authors thank Anastasia Kralli (Johns Hopkins University, Baltimore, MD, USA) for the *Ppargc1a*$^{flox/flox}$ and *Ppargc1b*$^{flox/flox}$ mice and helpful discussions. This work was supported by Grants SAF2011-23886 and SAF2012-39484 from Ministerio de Economía y competitividad (MINECO/FEDER; Spain) to J.A.V. and Grant PI15/00701 from Instituto de Salud Carlos III (ISCIII) to P.M.G.-R. The authors declare no conflicts of interest.

AUTHOR CONTRIBUTIONS

R. Pardo, M. Vilà, L. Cervela, M. de Marco, P. Gama-Pérez, A. González-Franquesa, and L. Statuto performed research and analyzed data; R. Vilallonga and R. Simó contributed with material/reagents and reviewed the drafted manuscript; P. M. Garcia-Roves designed research, analyzed data, contributed to the discussion, and reviewed the manuscript; and J. A. Villena conceived of and supervised the project, analyzed data, and wrote the paper.

REFERENCES

1. Guilherme, A., Virbasius, J. V., Puri, V., and Czech, M. P. (2008) Adipocyte dysfunctions linking obesity to insulin resistance and type 2 diabetes. *Nat. Rev. Mol. Cell Biol.* **9**, 367–377
2. International Diabetes Federation (2015) *IDF Diabetes Atlas*, International Diabetes Federation, Brussels, Belgium
3. Pellegrinelli, V., Carobbio, S., and Vidal-Puig, A. (2016) Adipose tissue plasticity: how fat depots respond differently to pathophysiological cues. *Diabetologia* **59**, 1075–1088
4. Lowell, B. B., and Shulman, G. I. (2005) Mitochondrial dysfunction and type 2 diabetes. *Science* **307**, 384–387
5. Chawla, A., Nguyen, K. D., and Goh, Y. P. (2011) Macrophage-mediated inflammation in metabolic disease. *Nat. Rev. Immunol.* **11**, 738–749
6. Wellen, K. E., and Hotamisligil, G. S. (2005) Inflammation, stress, and diabetes. *J. Clin. Invest.* **115**, 1111–1119
7. Bordone, L., and Guarente, L. (2005) Calorie restriction, SIRT1 and metabolism: understanding longevity. *Nat. Rev. Mol. Cell Biol.* **6**, 298–305
8. Zamora, M., and Villena, J. A. (2014) Targeting mitochondrial biogenesis to treat insulin resistance. *Curr. Pharm. Des.* **20**, 5527–5557
9. Eguchi, J., Wang, X., Yu, S., Kershaw, E. E., Chiu, P. C., Dushay, J., Estall, J. L., Klein, U., Maratos-Flier, E., and Rosen, E. D. (2011) Transcriptional control of adipose lipid handling by IRF4. *Cell Metab.* **13**, 249–259
10. Enguix, N., Pardo, R., González, A., López, V. M., Simó, R., Kralli, A., and Villena, J. A. (2013) Mice lacking PGC-1β in adipose tissues reveal a dissociation between mitochondrial dysfunction and insulin resistance. *Mol. Metab.* **2**, 215–226
11. Pardo, R., Enguix, N., Lasheras, J., Feliu, J. E., Kralli, A., and Villena, J. A. (2011) Rosiglitazone-induced mitochondrial biogenesis in white adipose tissue is independent of peroxisome proliferator-activated receptor γ coactivator-1α. *PLoS One* **6**, e26989
12. Lasheras, J., Vilà, M., Zamora, M., Riu, E., Pardo, R., Poncelas, M., Cases, I., Ruiz-Meana, M., Hernández, C., Feliu, J. E., Simó, R., García-Dorado, D., and Villena, J. A. (2016) Gene expression profiling in hearts of diabetic mice uncovers a potential role of estrogen-related receptor γ in diabetic cardiomyopathy. *Mol. Cell. Endocrinol.* **430**, 77–88
13. Huang, W., Sherman, B. T., and Lempicki, R. A. (2009) Systematic and integrative analysis of large gene lists using DAVID bioinformatics resources. *Nat. Protoc.* **4**, 44–57
14. Mootha, V. K., Lindgren, C. M., Eriksson, K. F., Subramanian, A., Sihag, S., Lehar, J., Puigserver, P., Carlsson, E., Ridderstråle, M., Laurila, E., Houstis, N., Daly, M. J., Patterson, N., Mesirov, J. P., Golub, T. R., Tamayo, P., Spiegelman, B., Lander, E. S., Hirschhorn, J. N., Altshuler, D., and Groop, L. C. (2003) PGC-1alpha-responsive genes involved in oxidative phosphorylation are coordinately downregulated in human diabetes. *Nat. Genet.* **34**, 267–273
15. Villena, J. A., Hock, M. B., Chang, W. Y., Barcas, J. E., Giguère, V., and Kralli, A. (2007) Orphan nuclear receptor estrogen-related receptor alpha is essential for adaptive thermogenesis. *Proc. Natl. Acad. Sci. USA* **104**, 1418–1423
16. Cantó, C., and Garcia-Roves, P. M. (2015) High-resolution respirometry for mitochondrial characterization of ex vivo mouse tissues. *Curr. Protoc. Mouse Biol.* **5**, 135–153
17. Villena, J. A. (2015) New insights into PGC-1 coactivators: redefining their role in the regulation of mitochondrial function and beyond. *FEBS J.* **282**, 647–672
18. Uldry, M., Yang, W., St-Pierre, J., Lin, J., Seale, P., and Spiegelman, B. M. (2006) Complementary action of the PGC-1 coactivators in mitochondrial biogenesis and brown fat differentiation. *Cell Metab.* **3**, 333–341
19. Fabbiano, S., Suárez-Zamorano, N., Rigo, D., Veyrat-Durebex, C., Stevanovic Dokic, A., Colin, D. J., and Trajkovski, M. (2016) Caloric restriction leads to browning of white adipose tissue through type 2 immune signaling. *Cell Metab.* **24**, 434–446
20. Reaven, E., Wright, D., Mondon, C. E., Solomon, R., Ho, H., and Reaven, G. M. (1983) Effect of age and diet on insulin secretion and insulin action in the rat. *Diabetes* **32**, 175–180
21. Wetter, T. J., Gazdag, A. C., Dean, D. J., and Cartee, G. D. (1999) Effect of calorie restriction on in vivo glucose metabolism by individual tissues in rats. *Am. J. Physiol.* **276**, E728–E738
22. Barger, J. L., Vann, J. M., Cray, N. L., Pugh, T. D., Mastaloudis, A., Hester, S. N., Wood, S. M., Newton, M. A., Weindruch, R., and Prolla, T. A. (2017) Identification of tissue-specific transcriptional markers of caloric restriction in the mouse and their use to evaluate caloric restriction mimetics. *Aging Cell* **16**, 750–760
23. Civitarese, A. E., Carling, S., Heilbronn, L. K., Hulver, M. H., Ukropcova, B., Deutsch, W. A., Smith, S. R., and Ravussin, E.; CALERIE Pennington Team. (2007) Calorie restriction increases muscle mitochondrial biogenesis in healthy humans. *PLoS Med.* **4**, e76
24. Higami, Y., Pugh, T. D., Page, G. P., Allison, D. B., Prolla, T. A., and Weindruch, R. (2004) Adipose tissue energy metabolism: altered gene expression profile of mice subjected to long-term caloric restriction. *FASEB J.* **18**, 415–417
25. Nisoli, E., Tonello, C., Cardile, A., Cozzi, V., Bracale, R., Tedesco, L., Falcone, S., Valerio, A., Cantoni, O., Clementi, E., Moncada, S., and Carruba, M. O. (2005) Calorie restriction promotes mitochondrial biogenesis by inducing the expression of eNOS. *Science* **310**, 314–317
26. Hancock, C. R., Han, D. H., Higashida, K., Kim, S. H., and Holloszy, J. O. (2011) Does calorie restriction induce mitochondrial biogenesis? A reevaluation. *FASEB J.* **25**, 785–791
27. López-Lluch, G., Hunt, N., Jones, B., Zhu, M., Jamieson, H., Hilmer, S., Cascajo, M. V., Allard, J., Ingram, D. K., Navas, P., and de Cabo, R. (2006) Calorie restriction induces mitochondrial biogenesis and bioenergetic efficiency. *Proc. Natl. Acad. Sci. USA* **103**, 1768–1773
28. Finley, L. W., Lee, J., Souza, A., Desquiret-Dumas, V., Bullock, K., Rowe, G. C., Procaccio, V., Clish, C. B., Arany, Z., and Haigis, M. C. (2012) Skeletal muscle transcriptional coactivator PGC-1α mediates mitochondrial, but not metabolic, changes during calorie restriction. *Proc. Natl. Acad. Sci. USA* **109**, 2931–2936
29. Gerhart-Hines, Z., Rodgers, J. T., Bare, O., Lerin, C., Kim, S. H., Mostoslavsky, R., Alt, F. W., Wu, Z., and Puigserver, P. (2007) Metabolic control of muscle mitochondrial function and fatty acid oxidation through SIRT1/PGC-1alpha. *EMBO J.* **26**, 1913–1923
30. Kelly, T. J., Lerin, C., Haas, W., Gygi, S. P., and Puigserver, P. (2009) GCN5-mediated transcriptional control of the metabolic coactivator PGC-1beta through lysine acetylation. *J. Biol. Chem.* **284**, 19945–19952

31. Jäger, S., Handschin, C., St-Pierre, J., and Spiegelman, B. M. (2007) AMP-activated protein kinase (AMPK) action in skeletal muscle via direct phosphorylation of PGC-1alpha. *Proc. Natl. Acad. Sci. USA* **104**, 12017–12022
32. Bruce, C. R., Anderson, M. J., Carey, A. L., Newman, D. G., Bonen, A., Kriketos, A. D., Cooney, G. J., and Hawley, J. A. (2003) Muscle oxidative capacity is a better predictor of insulin sensitivity than lipid status. *J. Clin. Endocrinol. Metab.* **88**, 5444–5451
33. Rong, J. X., Qiu, Y., Hansen, M. K., Zhu, L., Zhang, V., Xie, M., Okamoto, Y., Mattie, M. D., Higashiyama, H., Asano, S., Strum, J. C., and Ryan, T. E. (2007) Adipose mitochondrial biogenesis is suppressed in db/db and high-fat diet-fed mice and improved by rosiglitazone. *Diabetes* **56**, 1751–1760
34. Wilson-Fritch, L., Nicoloro, S., Chouinard, M., Lazar, M. A., Chui, P. C., Leszyk, J., Straubhaar, J., Czech, M. P., and Corvera, S. (2004) Mitochondrial remodeling in adipose tissue associated with obesity and treatment with rosiglitazone. *J. Clin. Invest.* **114**, 1281–1289
35. Boden, G., Homko, C., Mozzoli, M., Showe, L. C., Nichols, C., and Cheung, P. (2005) Thiazolidinediones upregulate fatty acid uptake and oxidation in adipose tissue of diabetic patients. *Diabetes* **54**, 880–885
36. Bogacka, I., Xie, H., Bray, G. A., and Smith, S. R. (2005) Pioglitazone induces mitochondrial biogenesis in human subcutaneous adipose tissue in vivo. *Diabetes* **54**, 1392–1399
37. Feige, J. N., Lagouge, M., Canto, C., Strehle, A., Houten, S. M., Milne, J. C., Lambert, P. D., Mataki, C., Elliott, P. J., and Auwerx, J. (2008) Specific SIRT1 activation mimics low energy levels and protects against diet-induced metabolic disorders by enhancing fat oxidation. *Cell Metab.* **8**, 347–358
38. Lagouge, M., Argmann, C., Gerhart-Hines, Z., Meziane, H., Lerin, C., Daussin, F., Messadeq, N., Milne, J., Lambert, P., Elliott, P., Geny, B., Laakso, M., Puigserver, P., and Auwerx, J. (2006) Resveratrol improves mitochondrial function and protects against metabolic disease by activating SIRT1 and PGC-1alpha. *Cell* **127**, 1109–1122
39. Nedergaard, J., and Cannon, B. (2013) UCP1 mRNA does not produce heat. *Biochim. Biophys. Acta* **1831**, 943–949
40. Barquissau, V., Léger, B., Beuzelin, D., Martins, F., Amri, E. Z., Pisani, D. F., Saris, W. H. M., Astrup, A., Maoret, J. J., Iacovoni, J., Déjean, S., Moro, C., Viguerie, N., and Langin, D. (2018) Caloric restriction and diet-induced weight loss do not induce browning of human subcutaneous white adipose tissue in women and men with obesity. *Cell Reports* **22**, 1079–1089
41. Cypess, A. M., Lehman, S., Williams, G., Tal, I., Rodman, D., Goldfine, A. B., Kuo, F. C., Palmer, E. L., Tseng, Y. H., Doria, A., Kolodny, G. M., and Kahn, C. R. (2009) Identification and importance of brown adipose tissue in adult humans. *N. Engl. J. Med.* **360**, 1509–1517
42. Hamann, A., Flier, J. S., and Lowell, B. B. (1996) Decreased brown fat markedly enhances susceptibility to diet-induced obesity, diabetes, and hyperlipidemia. *Endocrinology* **137**, 21–29
43. Himms-Hagen, J. (1985) Defective brown adipose tissue thermogenesis in obese mice. *Int. J. Obes.* **9** (Suppl 2), 17–24
44. Villarroya, F., Felipe, A., and Mampel, T. (1986) Brown adipose tissue activity in hypocaloric-diet fed lactating rats. *Biosci. Rep.* **6**, 669–675
45. Rothwell, N. J., and Stock, M. J. (1982) Effect of chronic food restriction on energy balance, thermogenic capacity, and brown-adipose-tissue activity in the rat. *Biosci. Rep.* **2**, 543–549
46. Pope, B. D., Warren, C. R., Parker, K. K., and Cowan, C. A. (2016) Microenvironmental control of adipocyte fate and function. *Trends Cell Biol.* **26**, 745–755
47. Henegar, C., Tordjman, J., Achard, V., Lacasa, D., Cremer, I., Guerre-Millo, M., Poitou, C., Basdevant, A., Stich, V., Viguerie, N., Langin, D., Bedossa, P., Zucker, J. D., and Clement, K. (2008) Adipose tissue transcriptomic signature highlights the pathological relevance of extracellular matrix in human obesity. *Genome Biol.* **9**, R14
48. Pasarica, M., Gowronska-Kozak, B., Burk, D., Remedios, I., Hymel, D., Gimble, J., Ravussin, E., Bray, G. A., and Smith, S. R. (2009) Adipose tissue collagen VI in obesity. *J. Clin. Endocrinol. Metab.* **94**, 5155–5162
49. Sun, K., Park, J., Gupta, O. T., Holland, W. L., Auerbach, P., Zhang, N., Goncalves Marangoni, R., Nicoloro, S. M., Czech, M. P., Varga, J., Ploug, T., An, Z., and Scherer, P. E. (2014) Endotrophin triggers adipose tissue fibrosis and metabolic dysfunction. *Nat. Commun.* **5**, 3485
50. Khan, T., Muise, E. S., Iyengar, P., Wang, Z. V., Chandalia, M., Abate, N., Zhang, B. B., Bonaldo, P., Chua, S., and Scherer, P. E. (2009) Metabolic dysregulation and adipose tissue fibrosis: role of collagen VI. *Mol. Cell. Biol.* **29**, 1575–1591
51. Reilly, S. M., and Saltiel, A. R. (2017) Adapting to obesity with adipose tissue inflammation. *Nat. Rev. Endocrinol.* **13**, 633–643
52. Park, C. Y., Park, S., Kim, M. S., Kim, H. K., and Han, S. N. (2017) Effects of mild calorie restriction on lipid metabolism and inflammation in liver and adipose tissue. *Biochem. Biophys. Res. Commun.* **490**, 636–642
53. Wang, Q., Perrard, X. D., Perrard, J. L., Mansoori, A., Raya, J. L., Hoogeveen, R., Smith, C. W., Ballantyne, C. M., and Wu, H. (2011) Differential effect of weight loss with low-fat diet or high-fat diet restriction on inflammation in the liver and adipose tissue of mice with diet-induced obesity. *Atherosclerosis* **219**, 100–108
54. Meydani, S. N., Das, S. K., Pieper, C. F., Lewis, M. R., Klein, S., Dixit, V. D., Gupta, A. K., Villareal, D. T., Bhapkar, M., Huang, M., Fuss, P. J., Roberts, S. B., Holloszy, J. O., and Fontana, L. (2016) Long-term moderate calorie restriction inhibits inflammation without impairing cell-mediated immunity: a randomized controlled trial in non-obese humans. *Aging (Albany N.Y.)* **8**, 1416–1431
55. Kang, K., Reilly, S. M., Karabacak, V., Gangl, M. R., Fitzgerald, K., Hatano, B., and Lee, C. H. (2008) Adipocyte-derived Th2 cytokines and myeloid PPARdelta regulate macrophage polarization and insulin sensitivity. *Cell Metab.* **7**, 485–495

Received for publication February 12, 2018.
Accepted for publication September 4, 2018.